Langmuir

ARTICLE

pubs.acs.org/Langmuir

In Situ Hydrolysis of Imine Derivatives on Au(111) for the Formation of Aromatic Mixed Self-Assembled Monolayers: Multitechnique Analysis of This Tunable Surface Modification

Ying Luo,[†] Matthias Bernien,[‡] Alex Krüger,[‡] Christian F. Hermanns,[‡] Jorge Miguel,[‡,§] Yin-Ming Chang,[‡] Simon Jaekel,[‡] Wolfgang Kuch,[‡] and Rainer Haag*[,†]

[†]Institut für Chemie und Biochemie, Freie Universität Berlin, Takustr. 3, 14195 Berlin, Germany

[‡]Institut für Experimentalphysik, Freie Universität Berlin, Arnimallee 14, 14195 Berlin, Germany

[§]Diamond Light Source, Harwell Science & Innovation Campus, OX11 0DE Chilton, Didcot, United Kingdom

Supporting Information

ABSTRACT: This paper presents a novel method for preparing aromatic, mixed self-assembled monolayers (SAMs) with a dilute surface fraction coverage of protonated amine via in situ hydrolysis of C═N double bond on gold surface. Two imine compounds, (4′-(4-(trifluoromethyl)benzylideneamino) biphenyl-4-yl)methanethiol ($CF_3-C_6H_4-CH═N-C_6H_4-C_6H_4-CH_2-SH$, **TFBABPMT**) and (4′-(4-cyanobenzylideneamino)biphenyl-4-yl)methanethiol ($CN-C_6H_4-CH═N-C_6H_4-C_6H_4-CH_2-SH$, **CBABPMT**), self-assembled on Au(111) to form highly ordered monolayers, which was demonstrated by infrared reflection absorption spectroscopy (IRRAS) and X-ray photoelectron spectroscopy (XPS). A nearly upright molecular orientation for CF_3- and CN-terminated SAM was detected by near edge X-ray absorption fine structure (NEXAFS) measurements. Afterward, the acidic catalyzed hydrolysis was carried out in chloroform or an aqueous solution of acetic acid (pH = 3). Systematic studies of this hydrolysis process for CN-terminated SAM in acetic acid at 25 °C were performed by NEXAFS measurements. It was found that about 30% of the imine double bonds gradually cleaved in the first 40 min. Subsequently, a larger hydrolysis rate was observed due to the freer penetration of acetic acid in the SAM and resultant more open molecular packing. Furthermore, the molecular orientation in mixed SAMs did not change during the whole hydrolysis process. This partially hydrolyzed surface contains a controlled amount of free amines/ammonium ions which can be used for further chemical modifications.

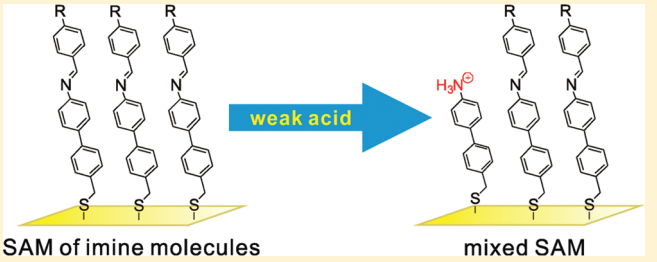

INTRODUCTION

Since the 1980s, the research on self-assembled monolayers (SAMs) on surfaces has attracted much attention. The controllable fabrication of organic molecules on metal surfaces, e.g., Au(111), alters the interface properties, thus making the surface applicable for catalysis, biosensing, and electronics.[1,2] In these SAMs, single thiol molecules are densely packed due to the strong interchain $\pi-\pi$ stacking or van der Waals interaction[3] and the chemical bond formations between the substrate gold and sulfur atoms.[4,5] Therefore, a highly ordered structure is normally observed.

In order to create surfaces with more complex functionalities, for instance, as biosensors or electronics devices, several different molecules have been lately employed in mixed SAMs, that modify not only the chemical but also the structure properties of the surface. Some methods for constructing the mixed SAMs have been presented.[6−12] Simultaneously, the surface properties and the corresponding applications have been studied as well.[13−20]

The first method, which is coadsorption, was introduced in 1989 by Whitesides and his colleagues.[6,13] Several mixed SAMs on gold were prepared by soaking chips in a mixed solution composed of two different alkanethiols. Relationships of the surface wettability to tail groups, solvents, and chain lengths were surveyed by means of contact angle measurements. Imaging and manipulating monolayers at nanoscale became possible after the development of modern experimental technology. The first systematic atomic force microscopy (AFM) study for *n*-alkanethiol mixed SAMs was performed in Hara's group.[14] The AFM image visually revealed the monolayer growth and the phase separation in the mixed SAMs. Apart from these examples of alkanethiols, Kang et al.[15−17] proved that the mixed SAMs of 4′-substituted-4-mercaptobiphenyls could also be established through coadsorption approach. They suggested that the

Received: July 14, 2011
Revised: November 23, 2011
Published: November 29, 2011

fractional surface coverage of the mixed SAMs might be related to the direction of the molecular dipole moments. Even though coadsorption is an universal method for mixed SAMs construction, the composition in a monolayer is often different than in solution, and phase separation is generally hard to predict.

At the beginning of this century, dissociative adsorption of asymmetric disulfide[7,19,20] was used to prepare mixed photoresponsive SAMs, in which more free space around the outermost azobenzene moiety was obtained. This allowed reversible molecular transformation via photoisomerization that is normally difficult to achieve in single-component SAMs.[20] Furthermore, Chen et al.[8] took advantage of the two methods mentioned above and coadsorbed asymmetrical and symmetrical disulfides on Au(111). The results revealed that mixed disulfides formed more homogeneous SAMs than the mixed thiols.

The third approach is different from the first two methods due to its two-step deposition process.[9] A pre-prepared chip possessing a densely packed SAM of one surfactant is immersed into a solution of the second surfactant to form a mixed SAM via ligand exchanges. The disadvantage of this method is that the displacement preferably takes place at the etch pits and the defect sites in the gold surface, resulting in the formation of molecular domains.

Irradiation promoted exchange reaction (IPER) is an extension of the third method and a way to prepare strongly heterogeneous mixed SAMs that contain components with different types of molecular chains, e.g., alkanethiol and biphenyl thiol.[10,11] In this method, electron irradiation of SAMs is performed, which leads to partial decomposition of molecules or distortion of the molecular conformation and orientation. These "destroyed" molecules are then replaced in the resultant ligand exchange procedure.

Chemical modification is also an effective and convenient means. For instance, Chapman et al.[12] introduced reactions of amines with a SAM that presented interchain carboxylic anhydride groups on gold to produce mixed SAMs for resisting the nonspecific absorption or realizing biospecific binding of proteins. However, this method is mainly used to establish a SAM with a 1:1 coverage ratio of two components. To some extent, the applications of such mixed SAMs are therefore restricted.

Although the above-described methods have been widely used, the surface coverage of different components cannot be well and flexibly controlled.[21] To solve these problems, novel strategies are still needed.

It is well-known that the coupling between aldehyde and amine can be readily carried out and that the produced imine compound undergoes hydrolysis under the acidic condition. Due to the easy manipulation and cleanliness of these two reactions, they gradually became used for surface modification. To our knowledge, the first paper about imine formation on gold surface was published by Horton Jr. et al.[22] in 1997, in which a novel method was presented for attaching enzymes and other receptor systems on gold via covalent bonding of amine derivatives with aldehyde-terminated SAMs. Based on this encouraging result, different biomolecules, e.g., DNA/RNA,[23,24] proteins,[25,26] and fluorescent dyes,[27] were soon thereafter immobilized on gold or silicon oxide surfaces for application in biosensor technology. Moreover, a nitro-substituted aromatic imine was attached on surfaces via this imine coupling protocol and a new nanopatterning system was established after selective molecular transformations resulted from X-ray irradiation.[28−30] More recently, Tauk et al. reported the dynamic covalent chemistry of imine condensation that was used as a tool to construct complex mixed

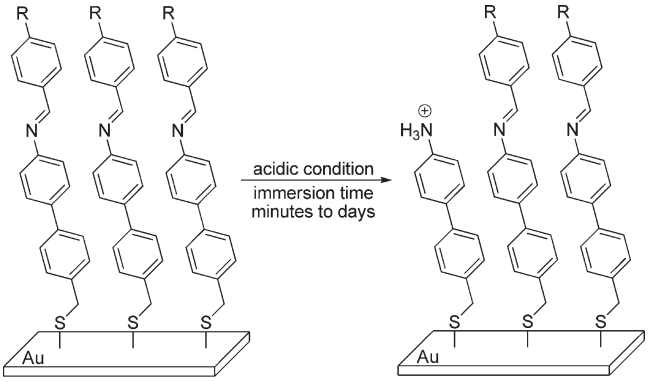

Figure 1. Idealized mixed SAMs on gold surface prepared by in situ hydrolysis of imine molecules under the acidic condition.

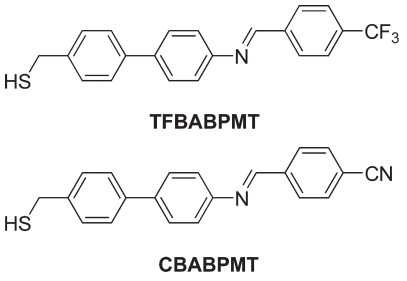

Figure 2. Chemical structures of two imine compounds **TFBABPMT** and **CBABPMT**.

gradients with a broad range of interfacial functionalities.[31] Besides the single-step coupling, stepwise synthesis of π-conjugated imine monolayer was also developed for preparing molecular electronics.[32−34] Previous works about hydrolysis of imine on surfaces, spectroscopic characterizations, and corresponding applications, however, were mainly performed in Reinhoudt's group.[27,35] They not only demonstrated the acid catalyzed cleavage of C═N double bonds on gold or silicon oxide surfaces but also achieved a directional movement of poly(propyleneimine) dendrimers on gradient glass surface based on the reversible imine formation.

In this study, we have taken advantage of the hydrolysis of aromatic imine compounds to form mixed SAMs possessing protonated amines with different coverage ratios (Figure 1). Amine functionalized mixed SAMs are particularly interesting for the studies of biomaterials due to their selective reactions with other complex functional groups.[36−39] However, no article has been reported on the hydrolysis process of imine bonds on surfaces to date. Most kinetics studies in SAMs were performed for hydrolysis of ester,[40−43] metal complexation,[44] and imine formation.[45,46] Additionally, unlike most of the application-related previously reported mixed SAMs,[47−49] in which molecules bearing active tail groups protrude over the "background" molecules, the mixed SAMs produced with our method expose ammonium ions in the depressed region due to the stiff backbones. This might be of interest to scientists for applications in the future.

The synthesis of two target aromatic imine compounds **TFBABPMT** and **CBABPMT** is introduced first in this paper (Figure 2). Then, we will discuss the preparation of their SAMs on gold surface and the characterizations using infrared reflection

dx.doi.org/10.1021/la202696a |*Langmuir* 2012, 28, 358–366

absorption spectroscopy (IRRAS), contact angle measurement, X-ray photoelectron spectroscopy (XPS), and near edge X-ray absorption fine structure (NEXAFS) for these monolayers. Acid-catalyzed hydrolysis of these imine functionalized SAMs by two methods as well as intensive investigation about the process of this two-dimensional reaction and the quality of the corresponding mixed SAMs by NEXAFS will be subsequently presented. In the final section, we will give a summary and conclusion for this work.

EXPERIMENTAL SECTION

General Methods. NMR spectra were recorded using a Delta 400 MHz instrument. High resolution mass measurements were run with Agilent 6210 ESI-TOF spectrometer. IR spectra for bulk materials were recorded on a Nicolet Avator 320 FT-IR spectrometer.

Reagents. All organic solvents, except for abs. ethanol from Merck, were purchased from Acros and used as received. The substrate 4′-aminobiphenyl-4-methanethiol for synthesizing imine compounds **TFBABPMT** and **CBABPMT** was prepared according to our previous work.[50] Two aldehydes 4-(trifluoromethyl) benzaldehyde and 4-cyanobenzaldehyde were obtained from Acros. The former was purified by distillation before every reaction, while the latter was directly used without any further purification.

Synthesis. *(a). TFBABPMT.* 4′-Aminobiphenyl-4-methanethiol (25.5 mg, 0.118 mmol) was dissolved in a solvent mixture of p.a. methanol (1.20 mL) and p.a. tetrahydrofuran (0.360 mL). Then, a solution of 4-(trifluoromethyl) benzaldehyde (21.0 mg, 0.118 mmol, 98%) in p.a. tetrahydrofuran (0.300 mL) was slowly added. The mixture was stirred at room temperature overnight under Ar. The solvents were removed under reduced pressure and additional silica gel column chromatography (chloroform/isopropanol 30:1 + 3% vol triethyl amine) gave a yellow powder with 34% yield. ^{1}H NMR (400 MHz, CD_2Cl_2): δ (ppm) 1.87 (t, ^3J (H, H) = 8 Hz, 1H; SH), 3.80 (d, ^3J (H, H) = 8 Hz, 2H; CH_2), 7.35 (d, ^3J (H, H) = 8 Hz, 2H; CH), 7.42 (d, ^3J (H, H) = 8 Hz, 2H; CH), 7.60 (d, ^3J (H, H) = 8 Hz, 2H; CH), 7.67 (d, ^3J (H, H) = 8 Hz, 2H; CH), 7.76 (d, ^3J (H, H) = 8 Hz, 2H; CH), 8.07 (d, ^3J (H, H) = 8 Hz, 2H; CH), 8.61 (s, 1H; CH); MS (ESI-TOF): m/z = 372.1024 ($[M+H]^+$, calcd. for $C_{21}H_{17}F_3NS^+$: 372.1028); IR (powder, cm^{-1}): ν = 1123, 1162, 1322, 1624, 2547.

(b). CBABPMT. Solvent abs. ethanol was degassed with Ar for 30 min. To a solution of 4′-aminobiphenyl-4-methanethiol (43.1 mg, 0.200 mmol) in pre-degassed abs. ethanol (9.00 mL), 4-cyanobenzaldehyde (27.0 mg, 0.200 mmol) in pre-degassed abs. ethanol (3.80 mL) was slowly added. The mixture was stirred at room temperature for 22 h under Ar. During the reaction, light yellow precipitate resulted, and after the reaction, these precipitates were collected via centrifugation and washed with abs. ethanol two times. Further removal of the solvents under vacuum gave a light yellow powder with 50% yield. ^{1}H NMR (400 MHz, CD_2Cl_2): δ (ppm) 1.87 (t, ^3J (H, H) = 8 Hz, 1H; SH), 3.80 (d, ^3J (H, H) = 8 Hz, 2H; CH_2), 7.35 (d, ^3J (H, H) = 8 Hz, 2H; CH), 7.42 (d, ^3J (H, H) = 8 Hz, 2H; CH), 7.60 (d, ^3J (H, H) = 8 Hz, 2H; CH), 7.67 (d, ^3J (H, H) = 8 Hz, 2H; CH), 7.79 (d, ^3J (H, H) = 8 Hz, 2H; CH), 8.05 (d, ^3J (H, H) = 8 Hz, 2H; CH), 8.59 (s, 1H; CH); MS (ESI-TOF): m/z = 329.1133 ($[M+H]^+$, calcd. for $C_{21}H_{17}N_2S^+$: 329.1107); IR (powder, cm^{-1}): ν = 1620, 2239, 2559.

Monolayer Preparation. Gold-coated glass (for IRRAS and contact angle measurements) and gold-coated mica (for XPS and NEXAFS) wafers were purchased from Arrandee and Georg Albert Physical Vapor Deposition, respectively. Au films on glass substrates were treated by piranha solution (3:1 mixture of concentrated sulfuric acid and 30% hydrogen peroxide) for 5 min at room temperature, subsequently rinsed with Millipore water and abs. ethanol for 1 min, and finally dried in an argon stream. On the other hand, Au films on mica substrates were purified by immersion in abs. ethanol for 10 min at room temperature, subsequently washed with abs. ethanol for 1 min, and then dried in an argon stream. The pretreated substrates were immersed in ethanolic solution of imine compound **TFBABPMT** or **CBABPMT** for 22 h under argon atmosphere at room temperature followed by annealing at 40 °C in abs. ethanol for two periods of 0.5 h each. Then, the sample was rinsed with p.a. acetonitrile, abs. ethanol, and dried with an argon stream.

In Situ Hydrolysis of Imine SAMs on Gold. The hydrolysis of imine compounds was carried out by immersion of gold chips presenting imine monolayer in p.a. chloroform (3 mL) at 30 °C (method a) or in an aqueous solution of acetic acid (pH = 3.0, 4.5 mL, method b) at 40 or 25 °C. After the reaction, the samples were rinsed with p.a. tetrahydrofuran (method a) or Millipore water (method b), abs. ethanol, and dried with argon.

Infrared Reflection Absorption Spectroscopy (IRRAS). Infrared reflection absorption spectra were measured using a nitrogen-purged NICOLET 8700 FT-IR spectrometer equipped with a liquid nitrogen cooled MCT detector. A molecular sieve filter device and a hydrophobic PEFT membrane made from active carbon were used to purify the nitrogen stream. All spectra were measured with a wavenumber resolution of 4 cm^{-1} and averaged over 2048 scans at an angle of incidence of 85° relative to the surface normal. The spectra are reported in absorbance units Log(1/R) after linear baseline correction. The spectrum of gold-coated glass washed with piranha solution for 5 min was used as reference.

Contact Angle Measurement. Static contact angles were measured on freshly prepared samples with a contact angle system OCA 20 from Dataphysics Instruments GmbH. Millipore water was used as the liquid for the drop formation. At least three drops at different locations on each sample were used.

Near Edge X-ray Absorption Fine Structure (NEXAFS). NEXAFS measurements were performed using synchrotron radiation from the bending magnet beamline PM3 at the storage ring BESSY II. Absorption spectra were acquired by total electron yield detection, recording the sample drain current as a function of photon energy. The spectra were normalized to the total electron yield of a freshly evaporated gold grid upstream to the experiment. Angle dependent measurements were carried out using p-polarized X-rays with 95% degree of polarization and angles of 20° (or 30°), 55°, and 90° between the incoming X-ray wavevector and the surface. Energy resolutions were set to 100 and 150 meV at the C and N-K edges, respectively. Calibration of the photon energy was carried out by NEXAFS measurements of gaseous N_2 and setting the position of the first N π^* resonance to 400.88 eV.[51] Typical photon flux densities of about 10^{13} s^{-1} cm^{-2} were used to prevent radiation damage. No change in the spectra with increasing illumination was observed for these flux densities. Test measurements with flux densities of about 10^{15} s^{-1} cm^{-2} showed a conversion of CF_3 groups to CF_2 deduced from the chemical shift of the C 1s XPS resonance after illumination for 1 h.

X-ray Photoelectron Spectroscopy (XPS). XPS measurements were performed using a Phoibos 100 electron energy analyzer from SPECS GmbH and X-rays from the synchrotron radiation of the bending magnet beamline PM3 at the storage ring BESSY II with photon energies of 385 and 260 eV for C 1s and S 2p XPS spectra, respectively. The electron takeoff angle was set to 0°, corresponding to normal emission. The binding energy is calibrated by referencing to the Au $4f_{7/2}$ resonance of the substrate at 84.0 eV measured for each photon excitation energy. Components in the XPS spectra were fitted by linear and Shirley backgrounds and pseudo Voigt functions. S 2p XPS spectra were fitted using S $2p_{3/2}$−S $2p_{1/2}$ doublets separated by 1.2 eV and an area ratio of 2:1.

RESULTS AND DISCUSSION

SAMs Preparation. Ethanol which was chosen in this experiment is a standard solvent applied for SAMs preparation.

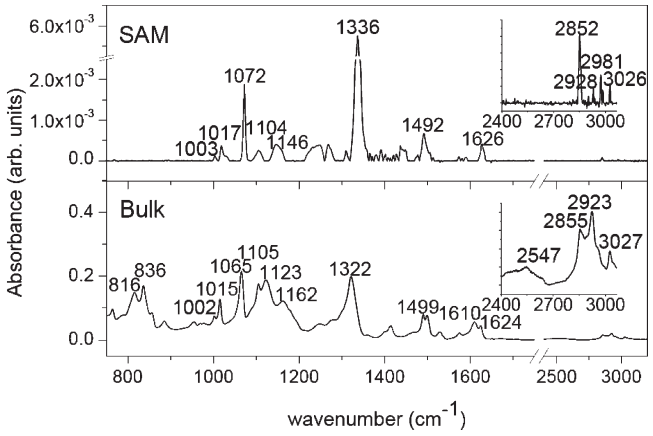

Figure 3. IR spectra of imine compound **TFBABPMT** in bulk (bottom) and in SAM on gold (top). Inset: amplification for high frequency region.

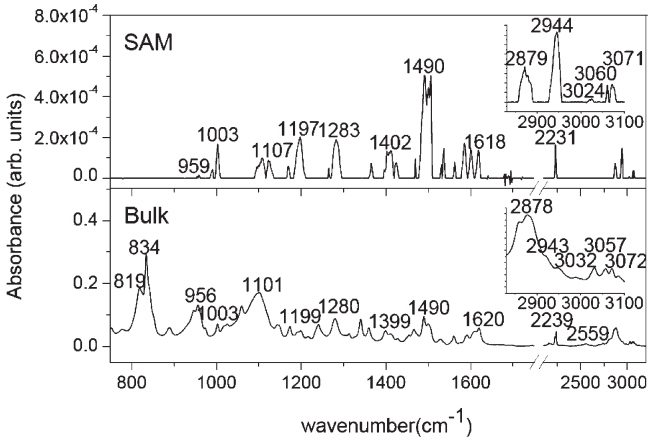

Figure 4. IR spectra of imine compound **CBABPMT** in bulk (bottom) and in SAM on gold (top). Inset: amplification for high frequency region.

However, the solubility of these two imine compounds in ethanol is not satisfactory. Therefore, their corresponding supersaturated ethanolic solutions were ultrasonicated for 10 min at room temperature, and then centrifuged at 4000 rpm for 10 min followed by filtration. UV−vis measurements were performed prior to the fabrication each time to confirm the reproducible concentration of the filtrate (**TFBABPMT**: ca. 0.05 mM, **CBABPMT**: ca. 0.1 mM, after dilution of the saturated solution). Subsequently, gold grafting was achieved as the procedure introduced in the Experimental Section.

IR Spectroscopy. IRRAS is a common method to acquire rough information about molecular structure and orientation in SAMs. Figure 3 and Figure 4 present the spectra in bulk and in SAM of imine compound **TFBABPMT** and **CBABPMT**, respectively. In general, the spectra in two different states are comparable, which initially suggests the presence of these two organic molecules on surfaces. For example, the peaks in the high frequency region from 2800 to 3100 cm^{-1} (Figures 3 and 4, inset) are assigned to C−H stretching of methylene group and phenyl ring. The other two peaks at ~1490 cm^{-1} and ~1003 cm^{-1} are associated with in-plane aromatic C═C vibrational mode and in-plane C−H bending in phenyl ring (Table 1). However, the vibration of 1,4-disubstituted

Table 1. Assignment of the Vibrational Modes Probed by IRRAS in Units of cm^{-1}[a]

	TFBABPMT		CBABPMT	
	Bulk	SAM	Bulk	SAM
ν(CH), ring	3027	3026	3032, 3057, 3072	3024, 3060, 3071
$\nu_{as}(CH_2)$	2923	2928	2878	2879
$\nu_{s}(CH_2)$	2855	2852		
ν(SH)	2547	---	2559	---
ν(C≡N)	/	/	2239	2231
ν(C═C), ring ip	1499	1492	1490	1490
$\nu_{s}(CF_3)$	1322	1336	/	/
$\nu_{as}(CF_3)$	1123, 1162	---	/	/
δ(CH), ring ip	1002	1003	1003	1003
δ(CH), ring op	816, 836	---	819, 834	---

[a] The abbreviations "ip" and "op" indicate in-plane and out-of-plane, respectively.

C−C stretching at ~1610 cm^{-1} cannot be easily identified on the spectra of SAMs, probably due to its weak absorbance and the influences of other peaks nearby, such as C═N stretching at ~1620 cm^{-1}.[52] All these results are consistent with the IR data reported for biphenyl-based thiols, *p*-terphenylthiol, and *p*-terphenylmethanethiol on gold surface.[53,54] Moreover, the observation of characteristic peaks for symmetric CF_3 stretching mode (1336 cm^{-1}, **TFBABPMT**) and C−N stretching mode (2231 cm^{-1}, **CBABPMT**) in the spectra of SAMs further indicated that SAMs formation of these two thiol compounds on gold surface was successful. Additional evidence for this argument is the signal disappearance of the S−H vibration in thiol group (**TFBABPMT**: 2547 cm^{-1}, **CBABPMT**: 2559 cm^{-1}) due to the dissociation of S−H single bond during the self-assembly process.[1] In addition, oxidized sulfur species (e.g., sulfone) that generally give rise to strong IR vibrations in the region range from 1130 to 1170 cm^{-1} were not observed, suggesting that no oxidation product appeared in SAMs.[55]

There are several striking changes in the spectra of SAMs when compared to bulk samples. First, in the bulk spectrum of **TFBABPMT** (Figure 3), the bands at 1123 and 1162 cm^{-1} are associated with the asymmetric CF_3 stretching mode, whose dipole moment is perpendicular to the molecular axis, with components both in and out of the aromatic ring plane.[56] The dramatic reduction of these two bands while in the spectrum of SAMs causes them to be buried by other peaks or even more likely to completely disappear. Second, in both cases (Figures 3 and 4), the bands at 816, 836, 819, and 834 cm^{-1} assigned as out-of-plane C−H wagging mode (Table 1) with a dipole moment orientated perpendicularly to the aromatic ring plane disappear as well.[57] The dramatic band intensity diminution and the absence of the bands imply that the transition dipole moments of $\nu_{as}(CF_3)$ and δ(CH) modes probably orientate parallel to the gold surface according to the surface selection rule. Therefore, it can be speculated that the molecules in SAMs are upright on the surface or slightly tilt to the surface normal.

In previous studies, we found that hydrolysis of imine derivatives in solution could be achieved without extra acidic reagents when chloroform was applied as the solvent due to the existence of a trace of hydrochloric acid inside it. So, the hydrolysis investigations of SAMs presenting CF_3 terminal groups were carried out first in chloroform at 30 °C. The IR spectra were recorded over time and

dx.doi.org/10.1021/la202696a |*Langmuir* 2012, 28, 358–366

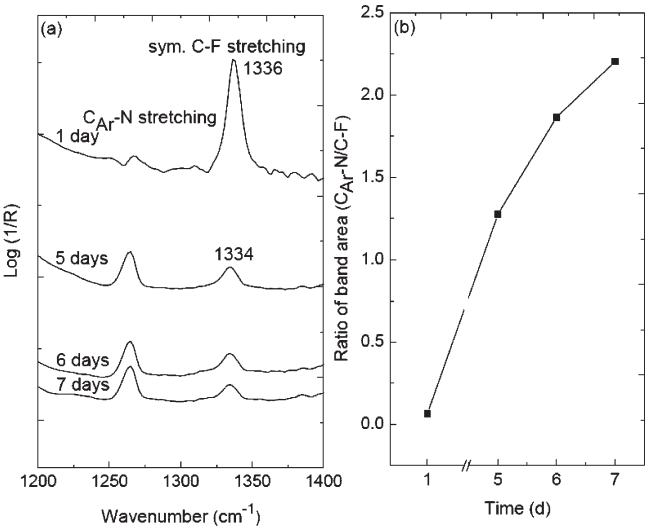

Figure 5. (a) IR spectra of CF_3-terminated SAMs in the range from 1200 cm^{-1} to 1400 cm^{-1} after hydrolysis in chloroform of 1 d, 5 d, 6 d, and 7 d. (b) Peak area ratio of $\nu(C_{Ar}N)$ to $\nu_s(CF_3)$ during hydrolysis.

are shown in Figure 5. Obviously, $\nu_s(CF_3)$ peak moderately reduced with an increase of the reaction time, and a concentration-dependent slight red shift from 1336 cm^{-1} to 1334 cm^{-1} was observed as well, which is supported by the research of Kang.[56] Furthermore, a new peak at 1265 cm^{-1} appeared and rapidly increased, which may be associated with the C_{Ar}-N stretching vibration from the aromatic primary amine produced. Similar results, the appearance of C_{Ar}-N stretching peak and an intensity decrease of $\nu(C{\equiv}N)$ peak, were also obtained in CN-terminated SAMs when the same hydrolysis condition was applied (IR spectra are not shown). The hydrolysis was not complete, however, even after one week owing to not enough acid in the chloroform. Therefore, acetic acid aqueous solution (pH = 3) was used instead. The hydrolysis reaction was performed at 40 °C and was usually completed within a few hours. The difference from the first method is that the peak of C−N stretching at ~1265 cm^{-1} was hardly observable probably because protonation of the amino group occurred in a relatively strong acidic condition and resulted in too few amino groups on the surface to be detected. Furthermore, it is encouraging that no bands of $\delta(CH)$ mode occurred after the hydrolysis process in both cases indicating that the molecular orientation in SAMs remained constant.

Contact Angle Measurements. Contact angle measurements were performed for monitoring the hydrolysis of SAMs in the aqueous solution of acetic acid at pH 3. Apparently, CF_3 group is much more hydrophobic compared to CN group so that a slower hydrolysis rate of the corresponding SAMs can be expected. Experiments were first carried out at 40 °C, and after 5 h, the contact angle of CF_3-terminated SAMs dropped from 100° to 22° (Figure 6a). In the case of SAMs presenting CN groups, however, the reaction rate was too fast to be recorded well under this condition. Therefore, the lower reaction temperature of 25 °C was used. The contact angle of this monolayer was reduced from 40° to 25° within 90 min (Figure 6b). Since the static water contact angle of amine-terminated SAMs is 62 ± 1° as reported by Pandey et al.,[58] protonated amine was therefore suggested as the product after the hydrolysis reaction in such cases.

X-ray Photoelectron Spectroscopy. High-resolution X-ray photoelectron spectroscopy (XPS) measurements of CF_3- and

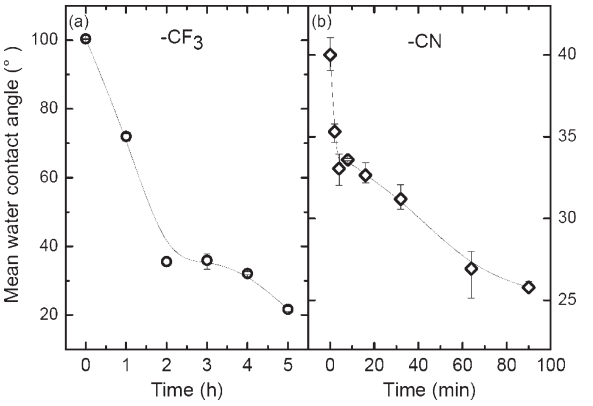

Figure 6. Static water contact angle during the hydrolysis of CF_3-terminated SAMs at 40 °C (a) and of CN-terminated SAMs at 25 °C (b) in acetic acid aqueous solutions with a pH value of 3.

CN-terminated SAMs on Au on mica were carried out to monitor the composition of the molecular layer. C 1s and S 2p XPS signals are plotted in Figure 7 over the binding energy for both SAMs. The binding energy of the individual C atoms within the molecule depends on their chemical environment, which leads to characteristic chemical shifts of the corresponding resonances in the XPS spectrum. In Figure 7a, the resonance at 291.9 eV can be attributed to the C atom of the CF_3 group. Since it terminates the SAM, its signal is not damped by overlying molecules. From the intensity ratio of the CF_3 resonance to the ones originating from the rest of the molecule of 0.24 ± 0.02 and the occurrence of the corresponding atoms in the molecule of 1:20, the damping constant a of the C signal can be evaluated according to

$$\frac{I_c(CF_3)}{I_c(\text{total})} = \frac{1 - e^{-a}}{e^{-a}(1 - e^{-20a})}$$

assuming a homogeneous distribution of C atoms in the SAM.[59] This leads to $a = 0.21 \pm 0.02$ per C atom along the molecule. The C 1s XPS signal of the cyano group (Figure 7b) displays a binding energy of 286.2 eV.[60] Its intensity ratio is 0.19 ± 0.02, which is similar to that of the CF_3-terminated SAM. The remaining intensity is characterized by two main resonances at 284.3 and 285.1 eV that can be attributed to aromatic C atoms in the phenyl rings. Since the cyano group is part of the conjugated system of the topmost phenyl ring, the signal of this carbon atom is shifted toward higher binding energies. The resonance positions of −CH═N− and −S−CH_2− cannot be unambiguously identified due to their small contribution to the C 1s XPS signal. For the CF_3-terminated SAM the C 1s resonance around 284.5 eV can be assigned to aromatic C. The N 1s XPS spectra (not shown) of the CF_3- and CN-terminated SAMs both display a single resonance at 398.5 and 399.2 eV binding energy, respectively. The difference in binding energy may be attributed to electrostatic effects in the photoemission process.[60] The contributions of the N atoms in the cyano and imine groups cannot be separated due to their almost identical chemical shifts.[61,62] In Figure 7c and d, S 2p XPS spectra are shown for the two SAMs.[63] In both cases, the spectrum is dominated by a S 2p doublet with the S $2p_{3/2}$ resonance at 162.1 eV. These doublets which correspond to sulfur groups bound to the gold surface prove the successful tethering of the molecules to the surface. A small contribution of sulfur with a $2p_{3/2}$ binding energy of 161.2 eV

dx.doi.org/10.1021/la202696a |*Langmuir* 2012, 28, 358–366

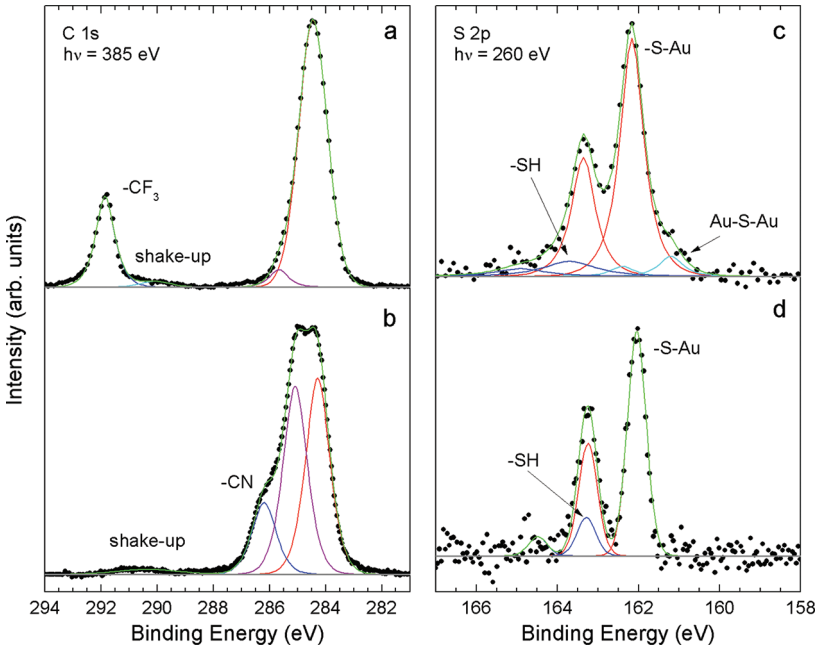

Figure 7. C 1s (left) and S 2p (right) XPS spectra of CF_3- (top) and CN- (bottom) terminated SAMs on Au/mica acquired with 385 and 260 eV photon energy.

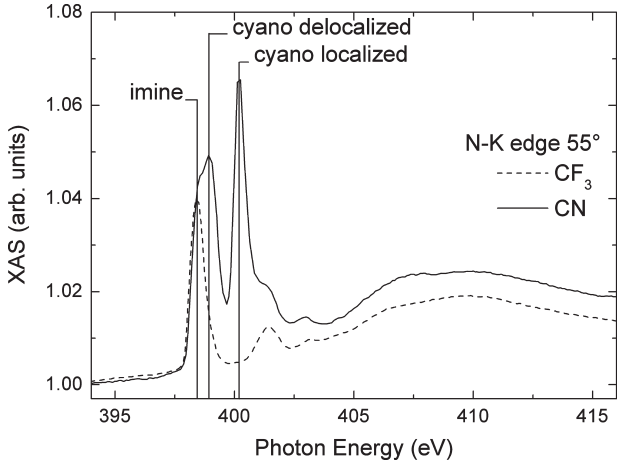

Figure 8. N−K NEXAFS spectra of CF_3- (dashed) and CN- (solid) terminated SAMs on Au/mica measured with *p*-polarized X-rays at an angle of incidence of 55° with respect to the surface (magic angle).

frequently assigned to atomic sulfur or highly coordinated sulfur[64] is observed for the CF_3-terminated SAM. Contributions of unbound thiol groups to the S 2p XPS signal can be identified at 163.3 eV. The intensity ratio of the unbound to bound sulfur groups is 0.14 and 0.17 for the CF_3- and CN-terminated SAM, respectively. Unbound molecules can either be incorporated in the SAM presumably by $\pi-\pi$ stacking or be loosely adsorbed on top of the SAM. The first case is unlikely because thiol-terminated SAMs show advancing and reducing contact angles of 67° and 62°,[56] which are very different from what we observed in the case of CF_3-terminated SAM (100°) and CN-terminated SAM (40°). For loosely adsorbed molecules, the S 2p XPS signal of the bound molecules is significantly damped. Since the kinetic energy of the photoelectrons is nearly the same as in the C 1s spectra, the same damping constant can be used

$$\frac{I_s(\mathrm{SH})}{I_s(\mathrm{SAu})} = \frac{N(\mathrm{SH})}{N(\mathrm{SAu})\cdot e^{-21a}}$$

where N(SH) and N(SAu) are the number of unbound and bound molecules, respectively. The resulting percentage of unbound molecules is below 1% in both cases. The XPS results show that for both types of molecules a well-defined SAM was formed with a negligible percentage of unbound molecules.

Near Edge X-ray Absorption Fine Structure. Near edge X-ray absorption fine structure (NEXAFS) spectroscopy probes the unoccupied molecular orbitals (MOs) in the vicinity of a certain element in the sample. It is therefore sensitive to the type of chemical bond of an element and its orientation. NEXAFS spectra at the N−K edge measured with p-polarized X-rays and an angle of 55° between the **k**-vector of the X-rays and the surface are presented for the CF_3- (dashed) and CN- (solid) terminated SAM (Figure 8). At this so-called magic angle the dependency of the NEXAFS signal on the orientations of the MOs cancels out. For the CF_3-terminated SAM, the only nitrogen contained in the molecules is the one within their imine bonds resulting in two π^* resonances at 398.4 and 401.4 eV photon energy. In addition to these resonances, two π^* resonances show up at 398.9 and 400.2 eV for the CN-terminated SAM. These resonances correspond to excitations into the cyano π^* MO oriented perpendicular and parallel to the plane of the phenyl ring, respectively.[65−67] The former orbital is delocalized over the phenyl ring, whereas the latter is localized at the cyano group. The orientations of these orbitals were determined by angle-dependent NEXAFS measurements at the N−K edge for the CN-terminated SAM (Figure 9). The corresponding spectra at the C−K edge and for the CF_3-terminated SAM are shown in Figures S1 and S2 of the Supporting Information. All π^* resonances of the CN-terminated SAM in the range of 398 to 402 eV photon energy display a pronounced dependence on the incidence angle of the X-rays. The average tilt

dx.doi.org/10.1021/la202696a |*Langmuir* 2012, 28, 358–366

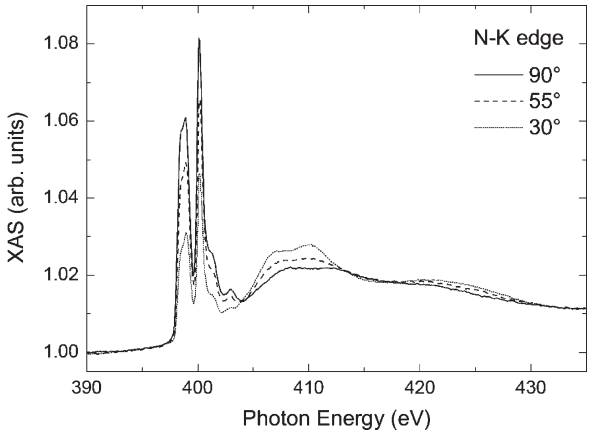

Figure 9. Angle-dependent N−K NEXAFS spectra of CN-terminated SAM on Au/mica measured with p-polarized X-rays.

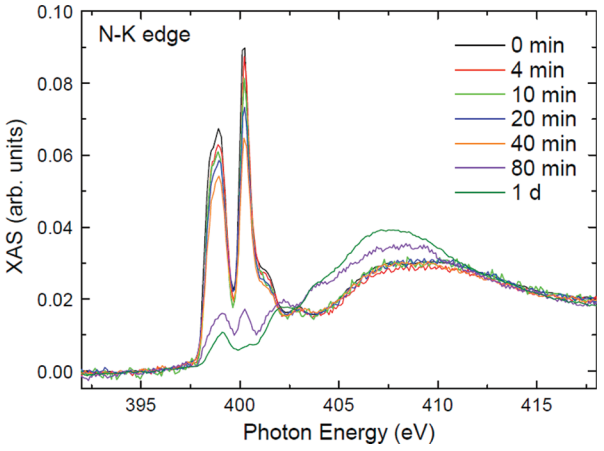

Figure 10. N−K edge NEXAFS spectra of the initial (black) CN-terminated SAM on Au/mica and after inlay into acetic acid of pH = 3 for increasing time measured with p-polarized X-rays at the magic angle.

Table 2. Average Tilt Angles of π Orbitals with Respect to the Surface Normal for the CF_3- and CN-Terminated SAM

CF_3-terminated SAM	
π^* phenyl	78° ± 5°
π^* imine	79° ± 3°
CN-terminated SAM	
π^* phenyl	67° ± 3°
π^* imine	70° ± 5°
cyano delocalized	68° ± 5°
cyano localized	65° ± 5°

angle of the MOs is obtained from the relative change in intensity of its corresponding resonance according to

$$I \propto 0.5(1-P)\sin^2\alpha + P(\cos^2\alpha\cos^2\theta + 0.5\sin^2\alpha\sin^2\theta)$$

where θ is the angle between the **k**-vector of the X-rays and the surface, α the angle between the axis of a vector-type orbital and the surface normal, and P the degree of linear polarization of the X-rays.[68] The obtained values for the two SAMs are given in Table 2. To infer the orientation of the molecules, the rotational freedom around their symmetry axis has to be considered. For orbitals perpendicular to this axis, the tilt angle β of the molecular axis with respect to the surface normal is connected to the tilt angle α of the orbital according to

$$\cos(\alpha) = \sin(\beta)\cos(\gamma)$$

where γ is the twist angle of the orbital with respect to the plane spanned by the surface normal and the symmetry axis of the molecule. The localized and delocalized π orbitals of the cyano group are oriented perpendicular to each other. This enables determination of the average twist and tilt angle of the upmost phenyl rings of the CN-terminated SAM from the two tilt angles of these orbitals[66] yielding an average tilt and twist angle of β = 34° ± 7° and γ = 48° ± 7°. Since the complete molecule is not rigid, an overall molecular twist and tilt angle cannot be assigned unambiguously. However, because the π orbitals of the phenyl rings and the one of the imine bond display average tilt angles similar to the cyano group, a straight arrangement of the molecule can be assumed with an average tilt of the molecular backbone of about 34° ± 7°. Assuming a twist angle of 48° for the CF_3-terminated SAM leads to an average tilt of the molecules of 17° ± 7°. This furthermore demonstrates the high degree of molecular order within the two SAMs.

In Situ Hydrolysis of Imine on Gold. Figure 10 shows the N−K edge NEXAFS spectra of CN-terminated SAMs after inlay of the SAM into acetic acid aqueous solution (pH = 3) for increasing time. All spectra were measured at the magic angle and normalized to the intensity of the X-rays by means of a reference signal from a gold grid upstream to the experiment. No normalization to the signal of the substrate (pre edge) was carried out. The resulting spectra can thus be compared to each other directly independent of the damping of the substrate signal and the orientation of the molecules.

Since the pK_a value of aromatic ammonium salt is about 3−5, a small amount of free amine might have been produced besides the protonated amino species ($-NH_3^+$) under the acidic condition (pH = 3) applied for this in situ hydrolysis. All imine double bonds in the SAM were cleaved after an inlay time of 1 d. The low intensity of the π^* resonance at 399.1 eV (dark green, Figure 10) may be attributed to excitations into the electronic system of the biphenyl rings which only have a small overlap with the core electrons of the nitrogen. This spectrum is similar to the one for monolayers self-assembled by the amine derivatives on gold surfaces, where acetic acid was also used in the preparation procedure.[69] The two resonances of the cyano group completely disappeared after 1 d, which proves that the cyano functionalized phenyl rings of the molecules were completely removed by the cleavage process. The resulting N−K spectrum is consistent with $-NH_3^+$ or $-NH_2$ termination of the cleaved SAM.[70]

The N−K edge spectra for intermediate time steps can be described by a superposition of the initial one and the one of the fully cleaved SAMs. The ratio of cleaved to complete molecules in the SAM is given by the relative weights of the two contributions to the spectra. The percentage of complete imine molecules in the SAM is plotted over the inlay time evaluated by the integration of the intensity of the localized cyano resonance between 399.2 and 401.3 eV photon energy (Figure 11). A gradual decrease of complete imine molecules was observed up to 40 min. Between 40 and 80 min, a sudden decrease in coverage became evident. Such behavior can be explained by the closely

dx.doi.org/10.1021/la202696a |*Langmuir* 2012, 28, 358–366

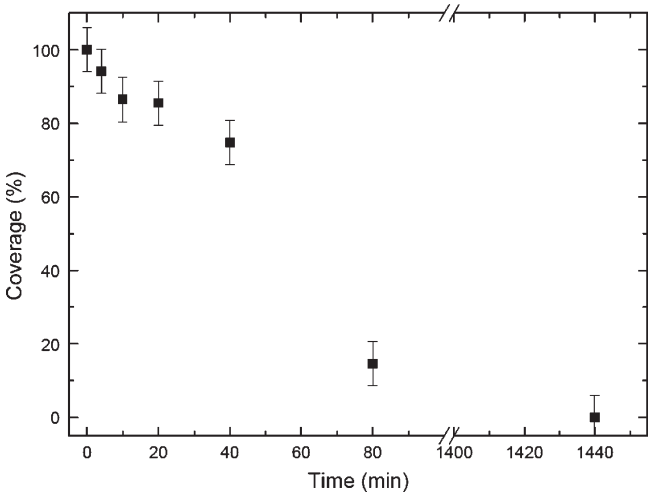

Figure 11. Relative coverage of the sample surface with CN-terminated imine molecules over inlay time in acidic solution obtained at 25 °C by integration of the NEXAFS intensity of the localized cyano resonance in the range of 399.2 to 401.3 eV photon energy.

packed molecules in the SAM which protect the imine bonds from the acidic solution. This results in a low initial cleavage rate taking place either stochastically over the whole SAM with a low probability or at domain boundaries or defect sites in the SAM exhibiting a more open molecular packing. Above a certain threshold, the acid could more freely penetrate the SAM and resulted in a sudden increase in cleavage rate. This situation may differ from SAMs grown on Au-covered glass substrates since their molecular arrangement is likely to be more open because of the higher surface roughness after cleaning with piranha solution. In this case, the faster hydrolysis rate might be due to the better accessibility of acid into the monolayer. The impact of the surface roughness at the atomic and the molecular scale on the ability of the imine SAMs to be hydrolyzed has not been studied, nor is it discussed in this paper. AFM measurements might solve this question in the future.

The same average tilting angles within the error bars are determined for the mixed SAMs obtained by hydrolysis from the angular dependence of the π^* resonances as for the initial SAM. The orientation of the biphenyl groups after an inlay time of one day could be obtained from the angle dependence of the C π^* resonance at 285.4 eV (SI Figure S3) and resulted in an average tilting angle of the molecular axis of 34° ± 7° if a twist angle of 48° is assumed. This shows that the high degree of orientational order of the initial SAMs was preserved during the whole hydrolysis process.

SUMMARY AND CONCLUSIONS

Self-assembly of two imine compounds **TFBABPMT** and **CBABPMT** on gold surfaces was achieved. These SAMs were characterized by IRRAS, XPS, NEXAFS, and contact angle measurements. It was demonstrated that densely packed and ordered monolayers were successfully obtained, and a nearly upright molecular orientation with an average tilt of 17° ± 7° and 34° ± 7° was determined by NEXAFS measurements for the CF_3- and CN-terminated SAM, respectively.

Moreover, in situ acidic catalyzed hydrolysis of imine groups in chloroform or acetic acid (pH = 3) was investigated in detail. Compared to the hydrolysis process that took several days in the former case, the same reaction was completed in just a few minutes to several hours when acetic acid was applied. NEXAFS studies for CN-terminated SAM in acetic acid showed that the cleavage rate of the reaction in the monolayer was correlated to the monolayer structure. In the first 40 min, the reaction was gradually carried out in the highly ordered, densely packed SAM and produced the mixed SAMs of protonated amine with a surface coverage about 0−30% based on the reaction time. Afterward, acid could readily penetrate the "decomposed" SAM, which gave a larger hydrolysis rate. Furthermore, NEXAFS measurements for mixed SAMs indicated that the molecular orientation remained constant and no free molecules were observed to lie on the top of the monolayer. Even though this surface modification is not a simple *n*th-order reaction and the rate constant is not given, in situ hydrolysis of imine bonds has been shown to be an alternate approach for preparing an aromatic mixed SAM with a dilute surface concentration of protonated amino group, which could have potential applications for partially positively charged surfaces or further chemical modification.

ASSOCIATED CONTENT

Supporting Information. Additional angle dependent NEXAFS spectra for CF_3-terminated SAM and for the CN-terminated SAM after an inlay time of 1 day in acetic acid solution included. This material is available free of charge via the Internet at http://pubs.acs.org.

AUTHOR INFORMATION

Corresponding Author

*E-mail: haag@chemie.fu-berlin.de. Tel: +49 (0)30 83852633. Fax: +49 (0)30 83853357.

ACKNOWLEDGMENT

Torsten Kachel is acknowledged for his technical support during the NEXAFS and XPS measurements. Kenji Yamamoto and Henryk Kalbe are acknowledged for preparatory experiments. Financial support by the DFG (Sfb 658) is gratefully acknowledged.

REFERENCES

(1) Ulman, A. *Chem. Rev.* **1996**, *96*, 1533–1554 and references herein.
(2) Love, J. C.; Estroff, L. A.; Kriebel, J. K.; Nuzzo, R. G.; Whitesides, G. M. *Chem. Rev.* **2005**, *105*, 1103–1170and references herein.
(3) Schwartz, D. K. *Annu. Rev. Phys. Chem.* **2001**, *52*, 107–137.
(4) Chailapakul, O.; Sun, L.; Xu, C.; Crooks, M. *J. Am. Chem. Soc.* **1993**, *115*, 12459–12467.
(5) Beibuyck, H. A.; Whitesides, G. M. *Langmuir* **1993**, *9*, 1766–1770.
(6) Bain, C. D.; Evall, J.; Whitesides, G. M. *J. Am. Chem. Soc.* **1989**, *111*, 7155–7164.
(7) Heister, K.; Allara, D. L.; Bahnck, K.; Frey, S.; Zharnikov, M.; Grunze, M. *Langmuir* **1999**, *15*, 5440–5443.
(8) Chen, S.; Li, L.; Boozer, C. L.; Jiang, S. *J. Phys. Chem. B* **2001**, *105*, 2975–2980.
(9) Lüssem, B.; Müller-Meskamp, L.; Karthäuser, S.; Waser, R.; Homberger, M.; Simon, U. *Langmuir* **2006**, *22*, 3021–3027.
(10) Ballav, N.; Weidner, T.; Rößler, K.; Lang, H.; Zharnikov, M. *ChemPhysChem* **2007**, *8*, 819–822.
(11) Ballav, N.; Terfort, A.; Zharnikov, M. *Langmuir* **2009**, *25*, 9189–9196.

(12) Chapman, R. G.; Ostuni, E.; Yan, L.; Whitesides, G. M. *Langmuir* **2000**, *16*, 6927–6936.
(13) Bain, C. D.; Whitesides, G. M. *J. Am. Chem. Soc.* **1989**, *111*, 7164–7175.
(14) Tamada, K.; Hara, M.; Sasabe, H.; Knoll, W. *Langmuir* **1997**, *13*, 1558–1566.
(15) Kang, J. F.; Liao, S.; Jordan, R.; Ulman, A. *J. Am. Chem. Soc.* **1998**, *120*, 9662–9667.
(16) Kang, J. F.; Jordan, R.; Ulman, A. *Langmuir* **1998**, *14*, 3983–3985.
(17) Kang, J. F.; Ulman, A.; Liao, S.; Jordan, R. *Langmuir* **1999**, *15*, 2095–2098.
(18) Lahiri, J.; Isaacs, L.; Grzybowski, B.; Carbeck, J. D.; Whitesides, G. M. *Langmuir* **1999**, *15*, 7186–7198.
(19) Noh, J.; Hara, M. *Langmuir* **2000**, *16*, 2045–2048.
(20) Akiyama, H.; Tamada, K.; Nagasawa, J.; Abe, K.; Tamaki, T. *J. Phys. Chem. B* **2003**, *107*, 130–135.
(21) Wink, T.; van Zuilen, S. J.; Bult, A.; van Bennekom, W. P. *Analyst* **1997**, *122*, 43R–50R.
(22) Horton, R. C., Jr.; Herne, T. M.; Myles, D. C. *J. Am. Chem. Soc.* **1997**, *119*, 12980–12981.
(23) Peelen, D.; Smith, L. M. *Langmuir* **2005**, *21*, 266–271.
(24) Rozkiewicz, D. I.; Brugman, W.; Kerkhoven, R. M.; Ravoo, B. J.; Reinhoudt, D. N. *J. Am. Chem. Soc.* **2007**, *129*, 11593–11599.
(25) Rozkiewicz, D. I.; Kraan, Y.; Werten, M. W. T.; de Wolf, F. A.; Subramaniam, V.; Ravoo, B. J.; Reinhoudt, D. N. *Chem.—Eur. J.* **2006**, *12*, 6290–6297.
(26) Rogero, C.; Chaffey, B. T.; Mateo-Martí, E.; Sobrado, J. M.; Horrocks, B. R.; Houlton, A.; Lakey, J. H.; Briones, C.; Martín-Gago, J. A. *J. Phys. Chem. C* **2008**, *112*, 9308–9314.
(27) Rozkiewicz, D. I.; Ravoo, B. J.; Reihoudt, D. N. *Langmuir* **2005**, *21*, 6337–6343.
(28) Moon, J. H.; Kim, K.-J.; Kang, T.-H.; Kim, B.; Kang, H.; Park, J. W. *Langmuir* **1998**, *14*, 5673–5675.
(29) La, Y.-H.; Jung, Y. J.; Kang, T.-H.; Ihm, K.; Kim, K.-J.; Kim, B.; Park, J. W. *Langmuir* **2003**, *19*, 9984–9987.
(30) La, Y.-H.; Jung, Y. J.; Kim, H. J.; Kang, T.-H.; Ihm, K.; Kim, K.-J.; Kim, B.; Park, J. W. *Langmuir* **2003**, *19*, 4390–4395.
(31) Tauk, L.; Schröder, A. P.; Decher, G.; Giuseppone, N. *Nat. Chem.* **2009**, *1*, 649–656.
(32) Rosink, J. J. W. M.; Blauw, M. A.; Geerligs, L. J.; van der Drift, E.; Rousseeuw, B. A. C.; Radelaar, S. *Langmuir* **2000**, *16*, 4547–4553.
(33) Klare, J. E.; Tulevski, G. S.; Nuckolls, C. *Langmuir* **2004**, *20*, 10068–10072.
(34) Ashwell, G. J.; Urasinska-Wojcik, B.; Phillips, L. J. *Angew. Chem., Int. Ed.* **2010**, *49*, 3508–3512.
(35) Chang, T.; Rozkiewicz, D. I.; Ravoo, B. J.; Meijer, E. W.; Reinhoudt, D. N. *Nano Lett.* **2007**, *7*, 978–980.
(36) Chuang, W.-H.; Lin, J.-C. *J. Biomed. Mater. Res., Part A* **2007**, *82A*, 820–830.
(37) Dong, S.; Roman, M. *J. Am. Chem. Soc.* **2007**, *129*, 13810–13811.
(38) Buxboim, A.; Bar-Dagan, M.; Frydman, V.; Zbaida, D.; Morpurgo, M.; Bar-Ziv, R. *Small* **2007**, *3*, 500–510.
(39) Azam, M. S.; Fenwick, S. L.; Gibbs-Davis, J. M. *Langmuir* **2011**, *27*, 741–750.
(40) Schönherr, H.; Chechik, V.; Stirling, C. J. M.; Vancso, G. J. *J. Am. Chem. Soc.* **2000**, *122*, 3679–3687.
(41) Vaidya, B.; Chen, J.; Porter, M. D.; Angelici, R. J. *Langmuir* **2001**, *17*, 6569–6576.
(42) Dordi, B.; Schönherr, H.; Vancso, G. J. *Langmuir* **2003**, *19*, 5780–5786.
(43) Whittle, T. J.; Leggett, G. J. *Langmuir* **2009**, *25*, 9182–9188.
(44) Banks, J. T.; Yu, T. T.; Yu, H. Z. *J. Phys. Chem. B* **2002**, *106*, 3538–3542.
(45) Yang, M.-H.; Biewer, M. C. *Tetrahedron Lett.* **2005**, *46*, 349–351.
(46) Wensink, H.; Benito-Lopez, F.; Hermes, D. C.; Verboom, W.; Gardeniers, H. J. G. E.; Reinhoudt, D. N.; van den Berg, A. *Lab Chip* **2005**, *5*, 280–284.
(47) Scheibler, L.; Dumy, P.; Boncheva, M.; Leufgen, K.; Mathieu, H.-J.; Mutter, M.; Vogel, H. *Angew. Chem., Int. Ed.* **1999**, *38*, 696–699.
(48) Yu, Q.; Chen, S.; Taylor, A. D.; Homola, J.; Hock, B.; Jiang, S. *Sens. Actuators, B* **2005**, *107*, 193–201.
(49) Maus, L.; Spatz, J. P.; Fiammengo, R. *Langmuir* **2009**, *25*, 7910–7917.
(50) Luo, Y.; Korchak, S.; Vieth, H.-M.; Haag, R. *ChemPhysChem* **2011**, *12*, 132–135.
(51) Sodhi, R. N. S.; Brion, C. E. *J. Electron Spectrosc. Relat. Phenom.* **1984**, *34*, 363–372.
(52) Marten, J.; Erbe, A.; Critchley, K.; Bramble, J. P.; Weber, E.; Evans, S. D. *Langmuir* **2008**, *24*, 2479–2486.
(53) Rong, H.-T.; Frey, S.; Yang, Y.-J.; Zharnikov, M.; Buck, M.; Wühn, M.; Wöll, C.; Helmchen, G. *Langmuir* **2001**, *17*, 1582–1593.
(54) Fuxen, C.; Azzam, W.; Arnold, R.; Witte, G.; Terfort, A.; Wöll, C. *Langmuir* **2001**, *17*, 3689–3695.
(55) Tour, J. M.; Jones, L., II; Pearson, D. L.; Lamba, J. J. S.; Burgin, T. P.; Whitesides, G. M.; Allara, D. L.; Parikh, A. N.; Atre, S. V. *J. Am. Chem. Soc.* **1995**, *117*, 9529–9534.
(56) Kang, J. F.; Ulman, A.; Jordan, R. *Langmuir* **1999**, *15*, 5555–5559.
(57) Kang, J. F.; Ulman, A.; Liao, S.; Jordan, R.; Yang, G.; Liu, G. *Langmuir* **2001**, *17*, 95–106.
(58) Pandey, L. M.; Pattanayek, S. K. *Appl. Surf. Sci.* **2011**, *257*, 4731–4737.
(59) Carlson, T. A. *Surf. Interface Anal.* **1982**, *4*, 125–134.
(60) Ballav, N.; Schüpbach, B.; Neppl, S.; Feulner, P.; Terfort, A.; Zharnikov, M. *J. Phys. Chem. C* **2010**, *114*, 12719–12727.
(61) Rosink, J. J. W. M.; Blauw, M. A.; Geerligs, L. J.; van der Drift, E.; Rousseeuw, B. A. C.; Radelaar, S. *Langmuir* **2000**, *16*, 4547–4553.
(62) Sato, Y.; Ye, S.; Haba, T.; Uosaki, K. *Langmuir* **1996**, *12*, 2726–2736.
(63) Please note that the spectrum in Figure 7c and d is recorded with an energy resolution of 700 and 500 meV, respectively.
(64) Chesneau, F.; Zhao, J.; Shen, C.; Buck, M.; Zharnikov, M. *J. Phys. Chem. C* **2010**, *114*, 7112–7119.
(65) Rangan, S.; Gallet, J.-J.; Bournel, F.; Kubsky, S.; Guen, K.; Le; Dufour, G.; Rochet, F. *Phys. Rev. B* **2005**, *71*, 1653181–12.
(66) Ballav, N.; Schüpbach, B.; Dethloff, O.; Feulner, P.; Terfort, A.; Zharnikov, M. *J. Am. Chem. Soc.* **2007**, *129*, 15416–15417.
(67) Piantek, M.; Miguel, J.; Krüger, A.; Navío, C.; Bernien, M.; Ball, D. K.; Hermann, K.; Kuch, W. *J. Phys. Chem. C* **2009**, *113*, 20307–20315.
(68) Stöhr, J.; Outka, D. A. *Phys. Rev. B* **1987**, *36*, 7891–7905.
(69) Deitrich, P. M.; Graf, N.; Gross, T.; Lippitz, A.; Krakert, S.; Schüpbach, B.; Terfort, A.; Unger, W. E. S. *Surf. Interface Anal.* **2010**, *42*, 1184–1187.
(70) Messer, B. M.; Cappa, C. D.; Smith, J. D.; Wilson, K. R.; Gilles, M. K.; Cohen, R. C.; Saykally, R. J. *J. Phys. Chem. B* **2005**, *109*, 5375–5382.